ISTITUTO NAZIONALE DI GEOFISICA E VULCANOLOGIA

Velocity profile report at the seismic station IV.VOBA – Vobarno (BS)

Report sul profilo di velocità sismica per il sito della stazione sismica IV.VOBA – Vobarno (BS)

Working Group: **Claudia MASCANDOLA** **Sara LOVATI** **Marco MASSA**	Date: Dicembre 2019
Subject: **Final report illustrating measurements, analysis and results for Vs profile at station IV.VOBA**	

Convenzione DPC-INGV 2019-21, All.B2- WP1, Task 2: "Caratterizzazione siti accelerometrici" (Coord.: G.Cultrera, F. Pacor)
Cite as: Working group INGV "Agreement DPC-INGV 2019-21, All.B2- WP1, Task 2", (2019). Velocity profile report at the seismic station *IV.VOBA– Vobarno*. http://hdl.handle.net/2122/12907

INDEX

1. **Introduction** 3

2. **Geophysical Investigations** 4

3. **Seismic Velocity Model** 16

4. **Conclusions** 22

References 24

Disclaimer and limits of use of information 25

Esclusione di responsabilità e limiti di uso delle informazioni 26

1. INTRODUCTION

In this report, we present the geophysical measurements and the results obtained in the framework of the 2019-2021 agreement between INGV and DPC, Allegato B2, WP1 - TASK 2: "Caratterizzazione siti accelerometrici" (Coord.: G. Cultrera, F. Pacor). In this report, the results for station IV.VOBA, belonging to the Italian National Seismic Network (RSN-INGV), are presented. The recording station is located in Val Sabbia (Southern Alps), specifically in the town of Vobarno that is part of the Brescia province.

Geophysical measurements consist in ambient-vibration measurements in both single-station and 2D array configuration that provide results in terms of resonance frequency of the soil deposits and in terms of dispersion curves of surface waves. These curves are inverted to obtain a shear-wave velocity (Vs) profile that is suitable for assigning the soil class according to the current Italian seismic code (NTC 2018) and the current Eurocode (EC8).

2. GEOPHYSICAL INVESTIGATIONS

Figure 1 shows the locations of the IV.VOBA seismic station (Latitude: 45.64292°; Longitude: 10.50355° WGS84, red point) and of the 2D array, whose stations are reported in yellow. The distance between IV.VOBA seismic station and the center of the 2D array (VOB1) is 15 m.
The seismic sensors were positioned in a circular geometry with a radius of 15 m, as shown in Figure 1. The corresponding geographic coordinates are reported in Table 1.

Figure 1: Map of the geophysical measurements performed at the IV.VOBA site. The yellow points are the nine stations of the 2D array in passive configuration. The red point indicates the IV.VOBA seismic station.

Station	Lat. [°]	Lon. [°]	El. [m]
VOB1	45.642827	10.503705	245
VOB2	45.642895	10.503845	245
VOB3	45.642810	10.503881	245
VOB4	45.642946	10.503736	245
VOB5	45.642714	10.503694	245
VOB6	45.642925	10.503614	245
VOB7	45.642837	10.503533	245
VOB8	45.642756	10.503571	245
VOB9	45.642743	10.503815	245

Table 1: geographic coordinates of the array stations (WGS84).

All stations of the array are equipped with Reftek-130 digitizer and Lennartz 3D-5s velocimetric sensors. The measurements were recorded in July and lasted about an hour and a half.

A view of the fieldwork is shown in Figure 2. The seismic sensors were positioned in a circular geometry in order to have a homogeneous azimuthal coverage that allows a better performance of the array techniques.

a)

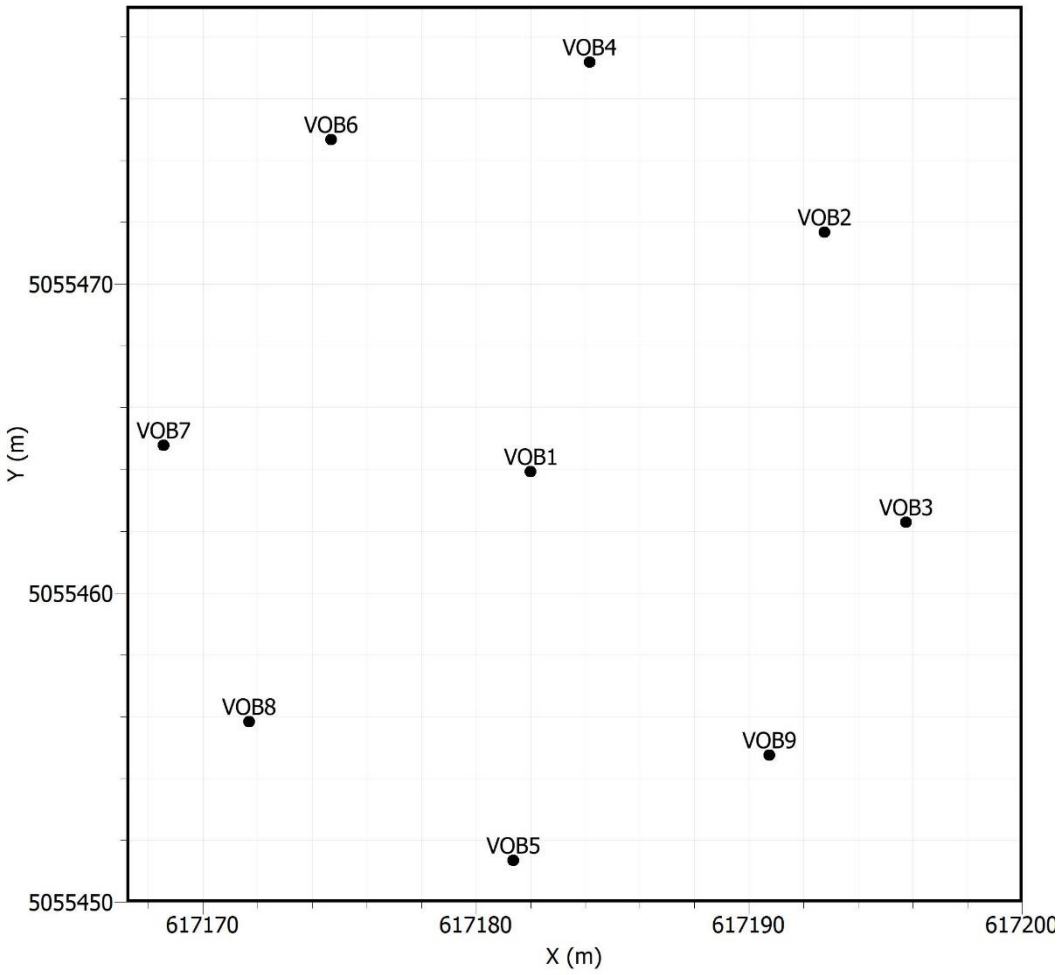

b)

Figure 2: a) fieldwork at the IV.VOBA seismic station. b) 2D array geometry (UTM coordinates).

The geometry of the array controls the response in terms of theoretical transfer function as described in Figure 3. On the left, the array transfer function is shown. On the right, the limits for the aliasing conditions are reported both in slowness and in velocity domains.

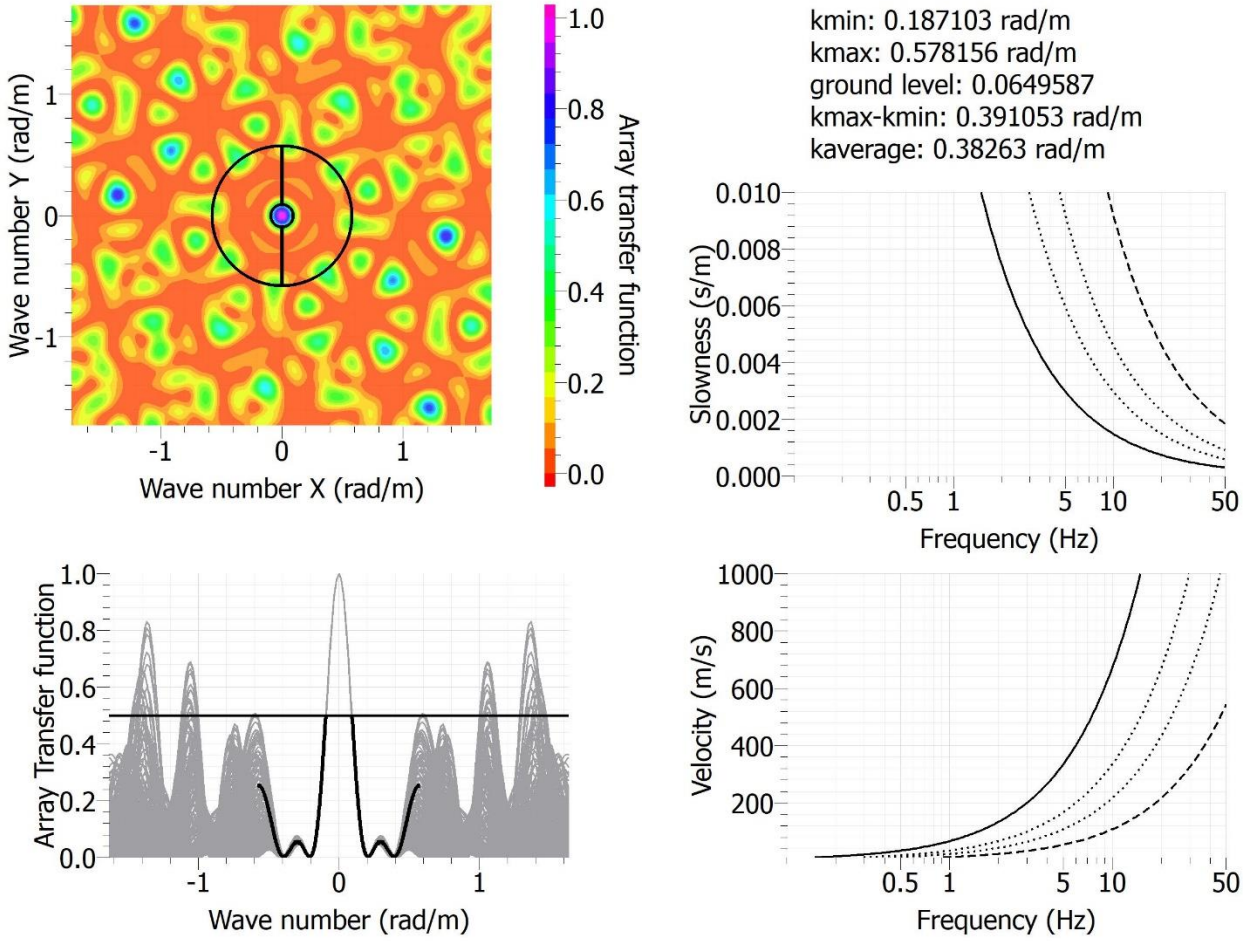

Figure 3: on the left, the theoretical array transfer function is reported for the 2D array. On the right, the aliasing conditions are reported in the slowness and velocity domains.

Figure 4 shows the H/V curves obtained from the 9 stations of the 2D array. The curves are superimposed on each other, indicating a peak at 5.5 Hz. At the same frequency, a polarization effect around 150° is observed on the rotated H/Vs in Figure 5. This effect is more evident for those seismic stations where the H/V peak is clear (VOB6, VOB7, VOB8).

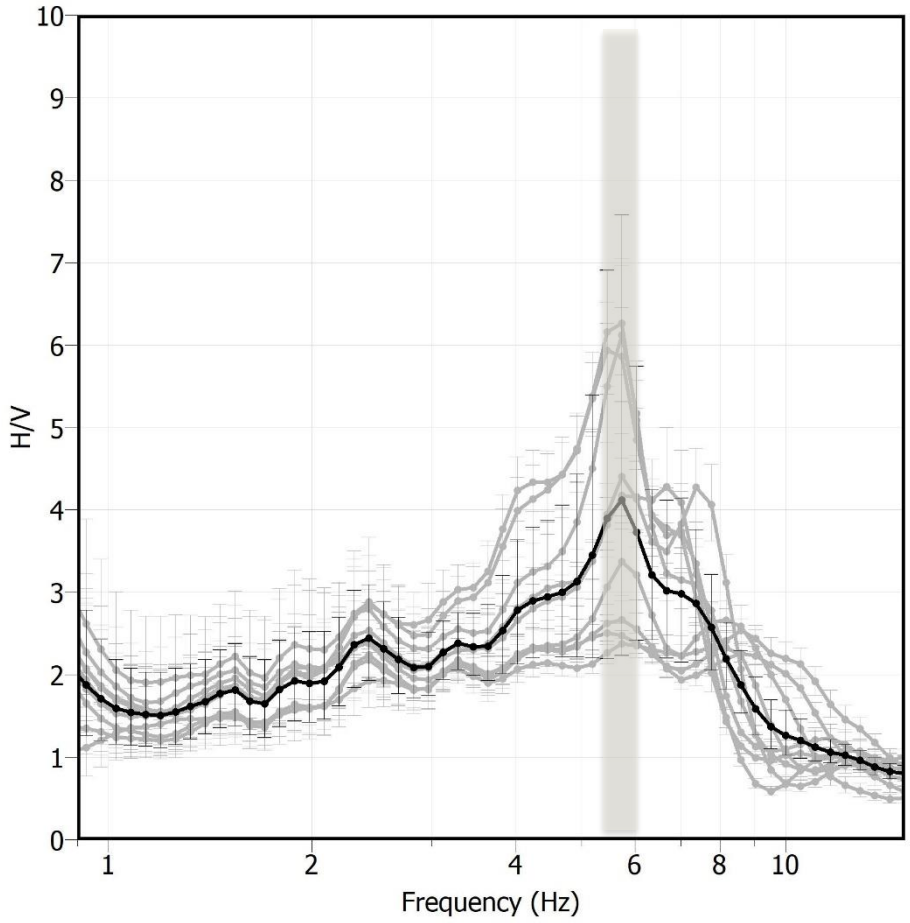

Figure 4: H/V curves of the 9 stations of the 2D array (in grey). The black curve is the average one. The vertical bars estimate the H/V uncertainties.

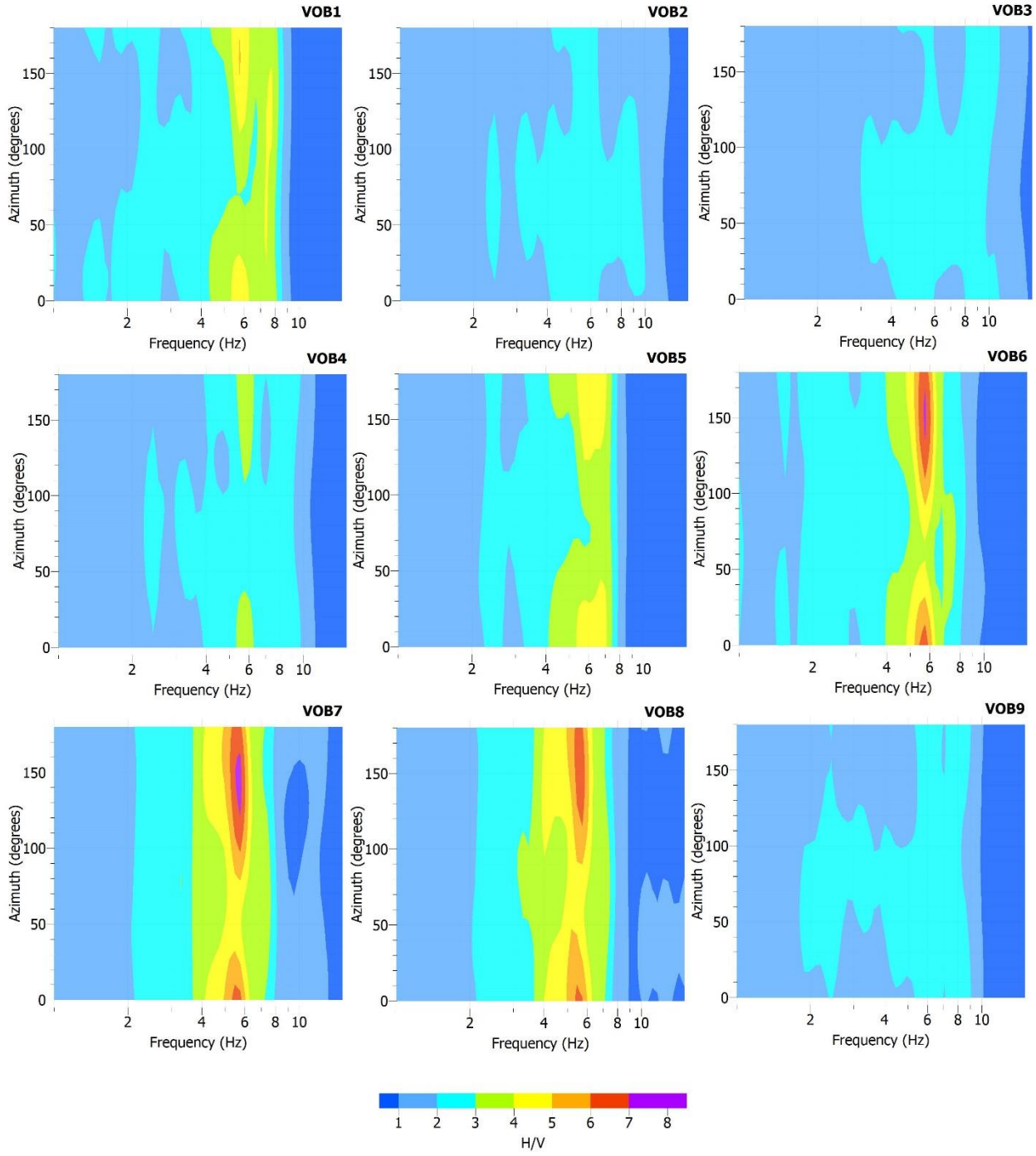

Figure 5: rotated H/V curves for the 9 stations of the 2D array.

The H/V results from the array recordings are in agreement with those obtained in the framework of the INGV-CRISP project (2015-2016) in correspondence to the IV.VOBA seismic station. In that case, a temporary ambient-vibration measurement was performed near the strong-motion station of IV.VOBA, reporting the H/V results in Figure 6. Figure 6a highlights a clear peak at 5.5 Hz, whereas Figure 6b indicates a polarization effect between 80° and 160°.

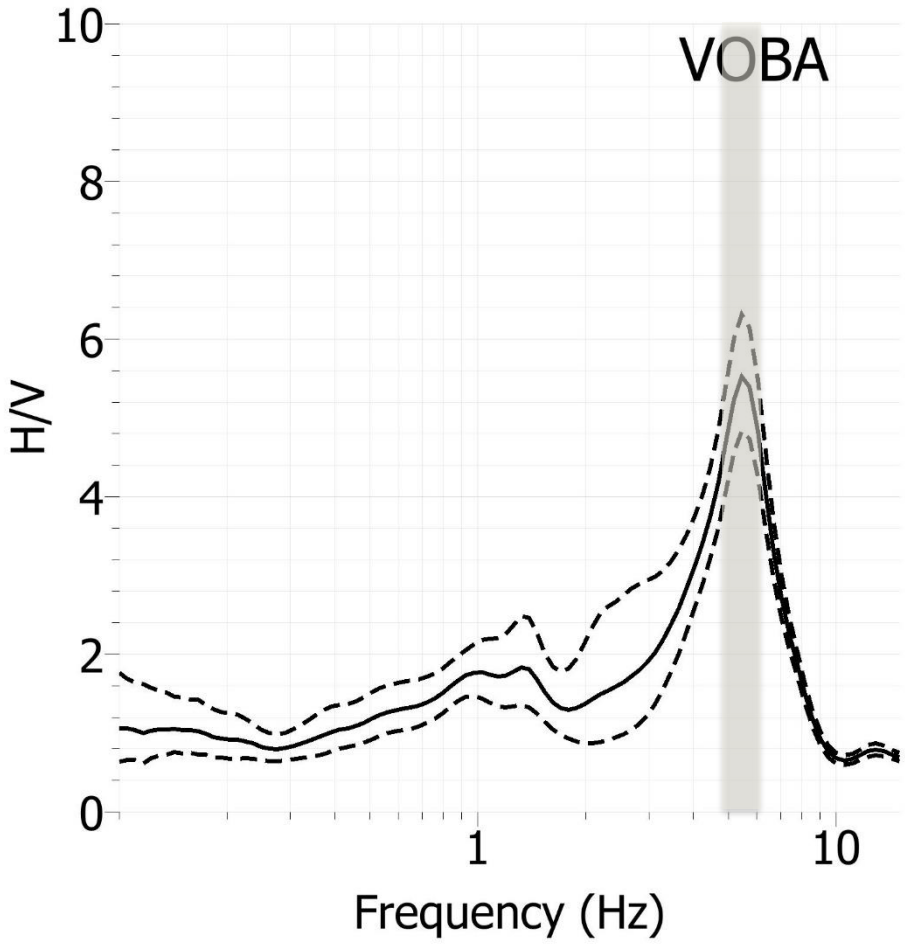

a)

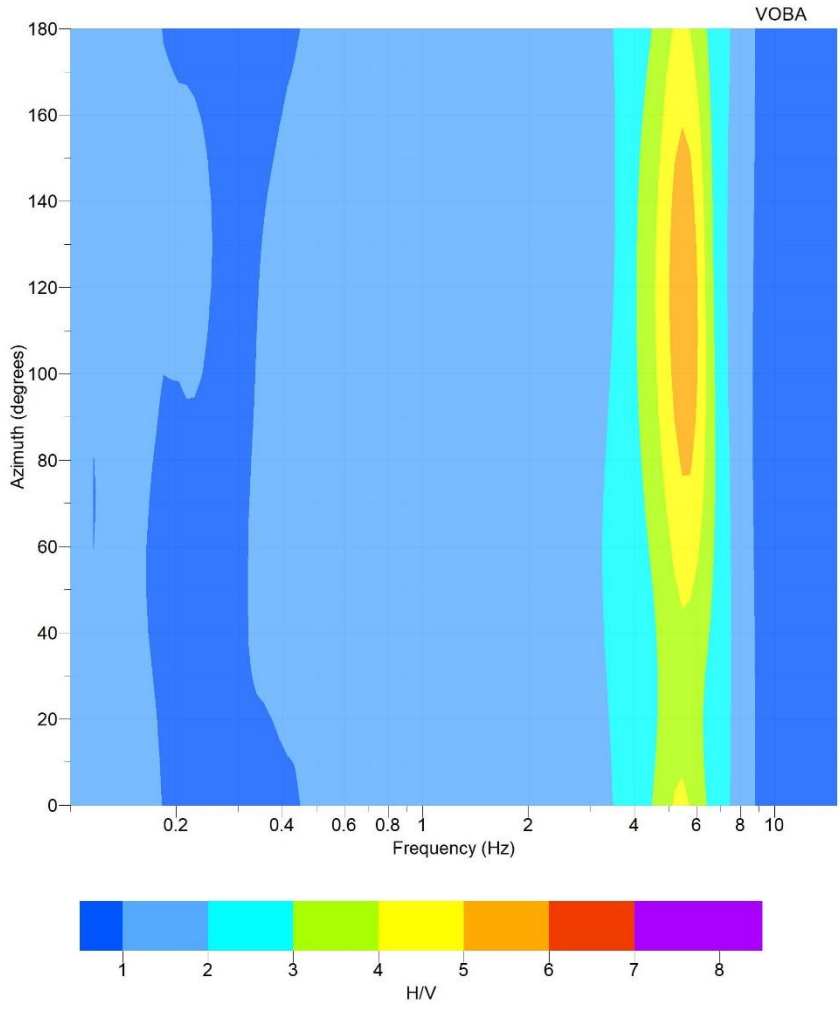

b)

Figure 6: a) H/V curve (mean: black solid line, standard deviation: black dashed lines) and b) rotated H/V at the IV.VOBA station.

Data from the 2D array have been analyzed with the GEOPSY code (http://www.geopsy.org) in terms of high-resolution FK analysis. The dispersion curve obtained from the vertical components is shown in Figure 7. We interpret and assume that the dispersion curve obtained in Figure 7 is relative to the fundamental mode of the Rayleigh dispersive waves. The aliasing conditions (black lines) constrain the validity range of the picked dispersion curves in the frequency range 10-20 Hz.

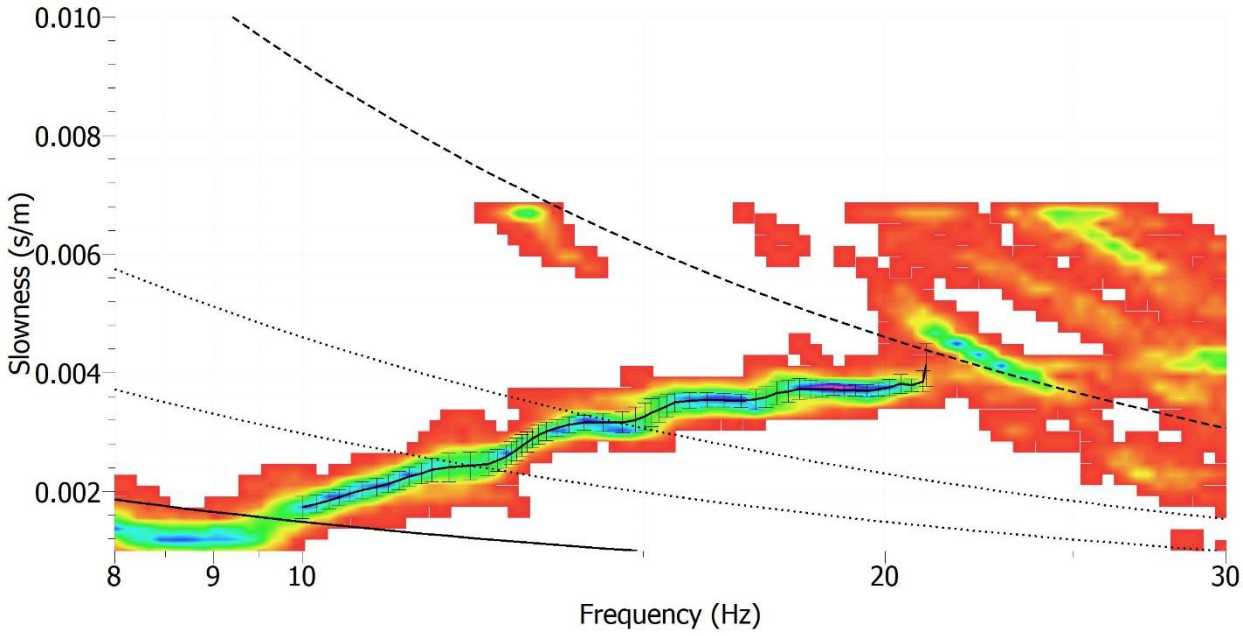

Figure 7: Picked dispersion curve in the slowness domain with the high-resolution FK analysis on the vertical components. The limits for the aliasing conditions are reported with black lines.

The modified spatial autocorrelation technique (MSPAC) has also been applied to the passive data to obtain the autocorrelation curves. Figure 8a shows the 7 rings adopted for the MSPAC analysis, whose geometries are reported in Table 2. Figure 8b shows the spatial autocorrelation curves computed for each ring.

Ring	R min	R max	Pairs
1	9.04	9.97	5
2	10.21	13	6
3	13.08	13.85	5
4	17.05	18.88	5
5	19.07	23.39	5
6	24.26	24.9	5
7	25.15	27.29	5

Table 2: geometry of the 7 rings adopted for the MSPAC analysis.

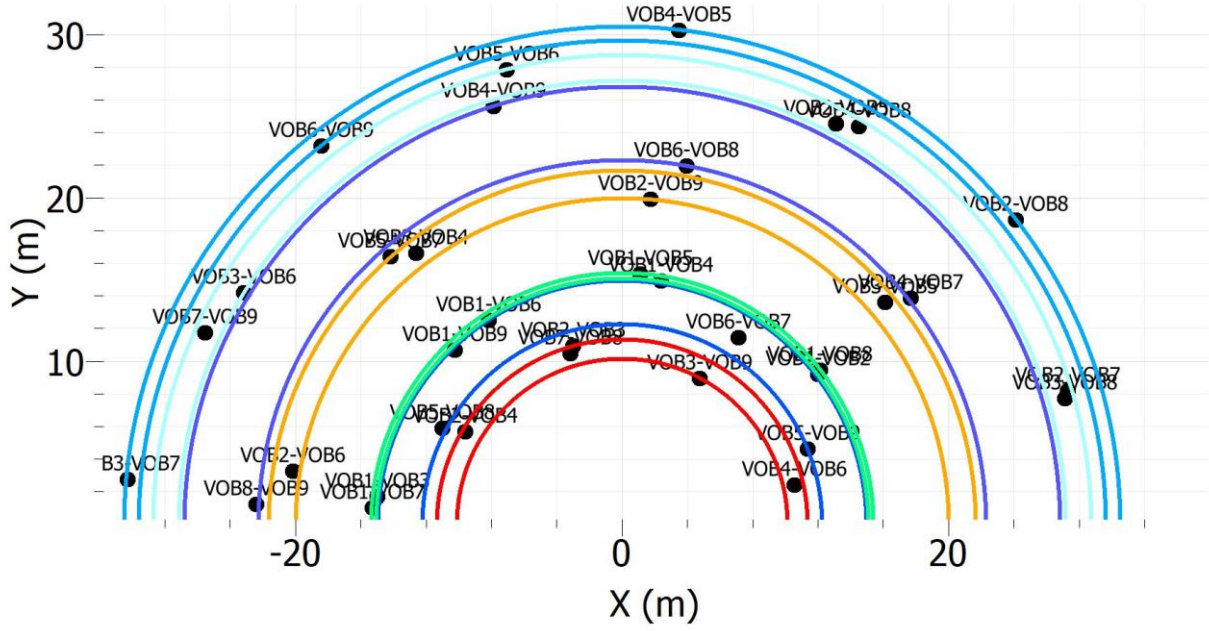

a)

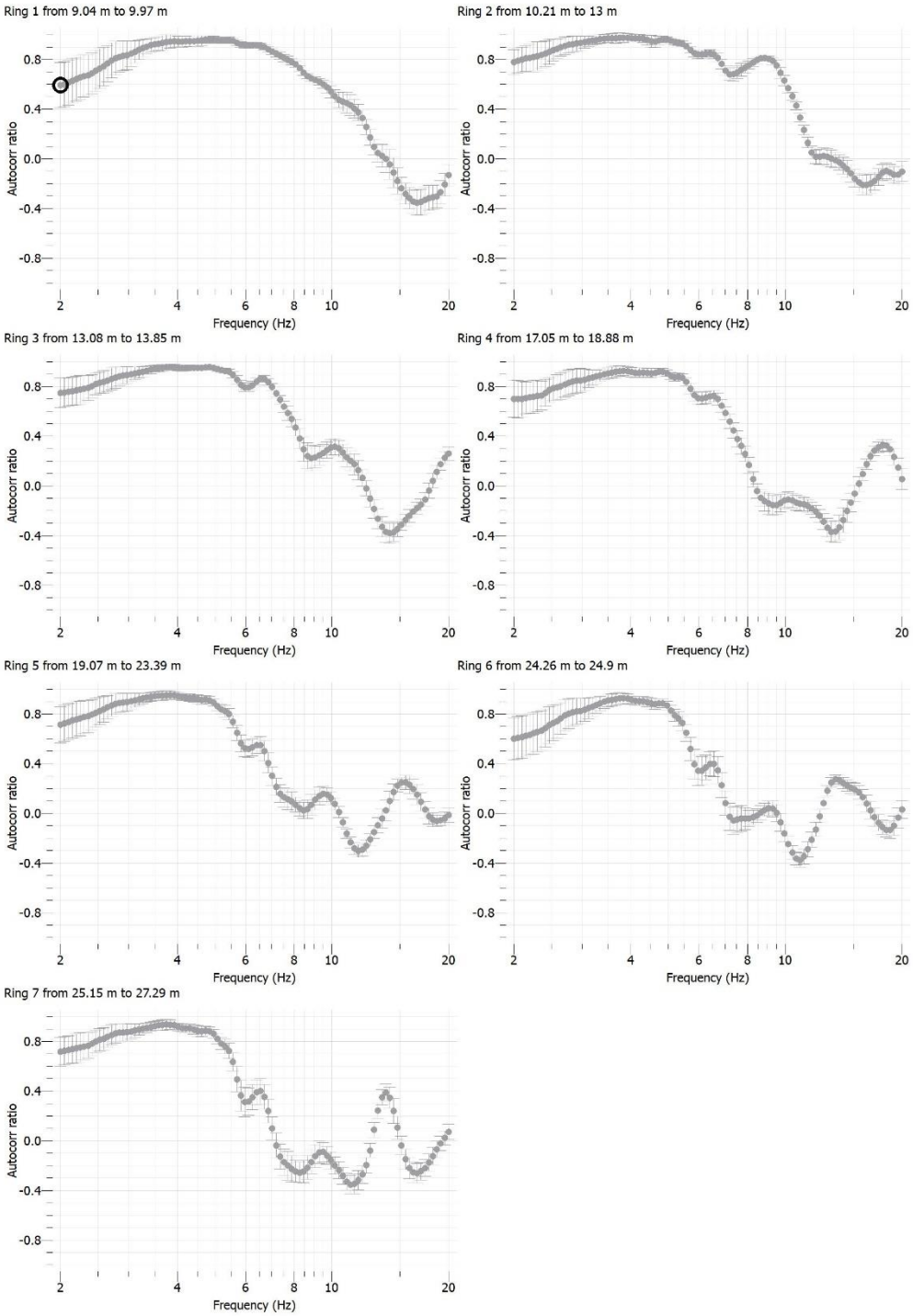

b)

Figure 8: a) rings selected for the MSPAC analysis; b) autocorrelation curves of the 7 rings.

The auto-correlation curves in Figure 8b have been inverted to obtain the corresponding dispersion curve (Figure 9) that we assume as relative to the fundamental mode of the Rayleigh dispersive waves in the frequency range 4-20 Hz.

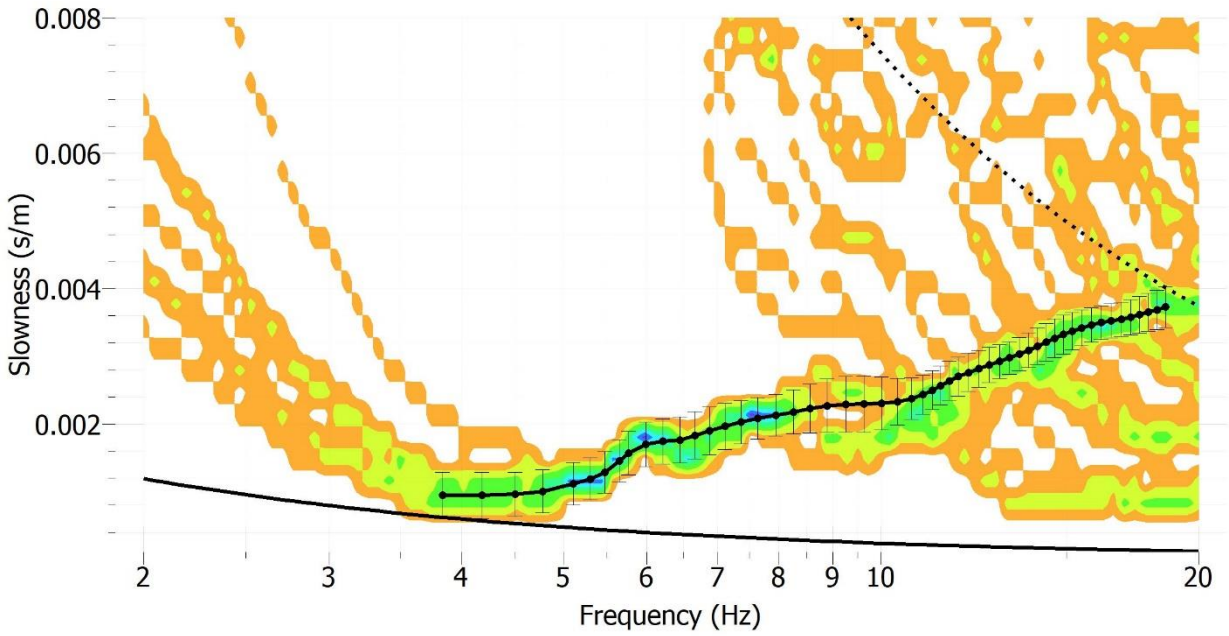

Figure 9: picked dispersion curve in the slowness domain with the MSPAC method.

3. SEISMIC VELOCITY MODEL

Figure 10a compares the dispersion curves obtained from the FK and MSPAC analyzes. A good correspondence is observed between 13 Hz and 18 Hz. At lower frequency (< 13 Hz), the FK dispersion curve is in a lower confidence range and it decays with respect to the MSPAC dispersion curve. The final curve, adopted for the inversion process, is shown in Figure 10b.

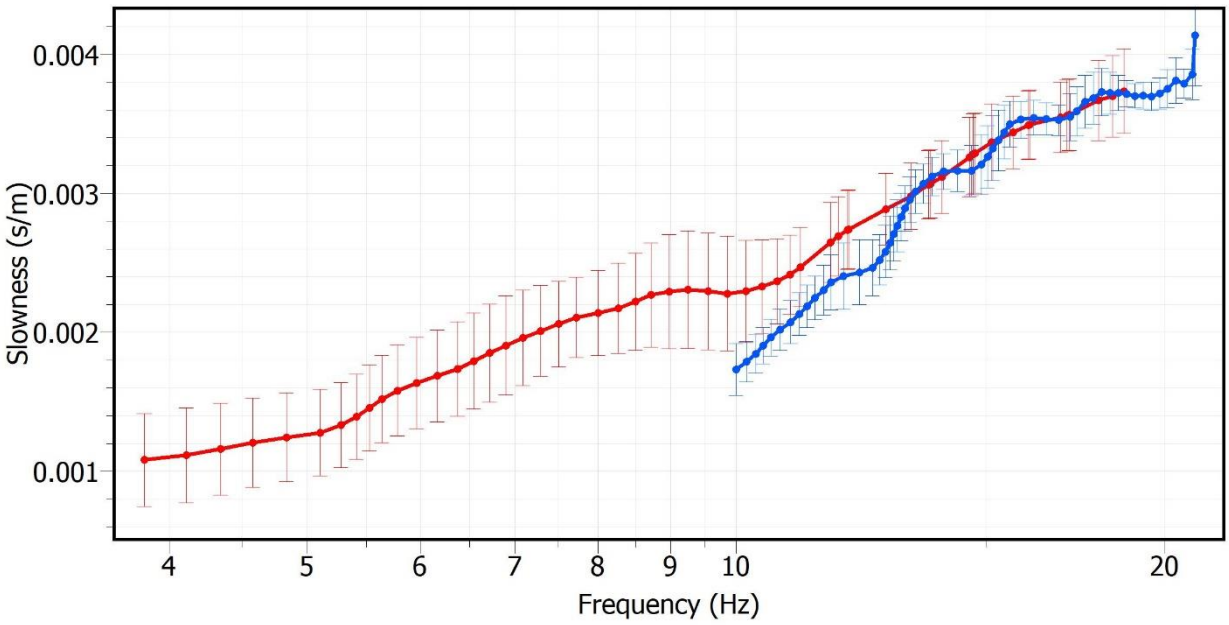

a)

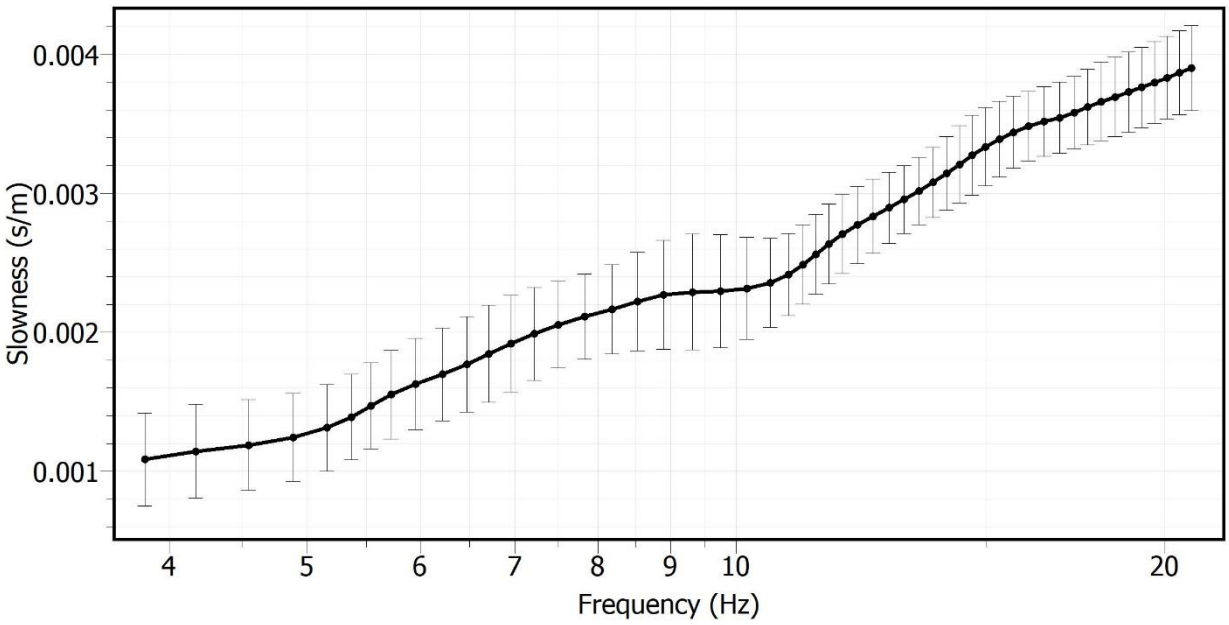

b)

Figure 10: a) Superimposed FK (blue) and MSPAC (red) dispersion curves in their validity limits. b) Dispersion curve adopted for the inversion process.

To proceed with the inversion, we estimate the ellipticity curve from the average H/V curve, considering in particular the right flank of the H/V peak that carries the important information on the underground structure. However, to reproduce the H/V peak we consider also the left flank. To reduce the contribution of the other waves in the H/V flanks, a common practice consists in reducing the H/V amplitude for the square root of 2 (Foti et al., 2011). The estimated ellipticity curve is reported in Figure 11 (blue curves) together with the average H/V curve (black curve).

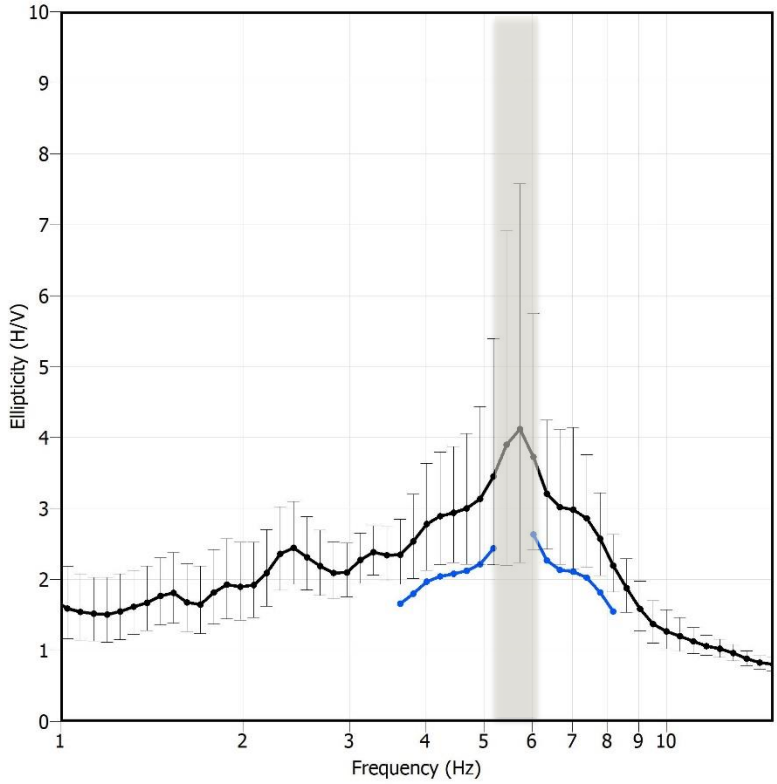

Figure 11: estimation of the ellipticity curve (blue) from the average H/V curve (black). The vertical bars estimate the H/V uncertainties.

Finally, we jointly invert the following targets:

1) Rayleigh wave dispersion curve (fundamental mode) in Figure 10b
2) ellipticity curve in Figure 11 (blue curve)

The resulting models after the inversion step are shown in Figure 12. We obtained a fairly good fit between experimental and theoretical curves using a model parameterization composed of three main layers over halfspace. Focusing on the *Vs* model of Figure 12, the results indicate soft layers (Vs ≤ 300) down to 8 m in depth, where *Vs* around 536 m/s are observed. The halfspace is found at 25 m in depth with Vs > 800 m/s.

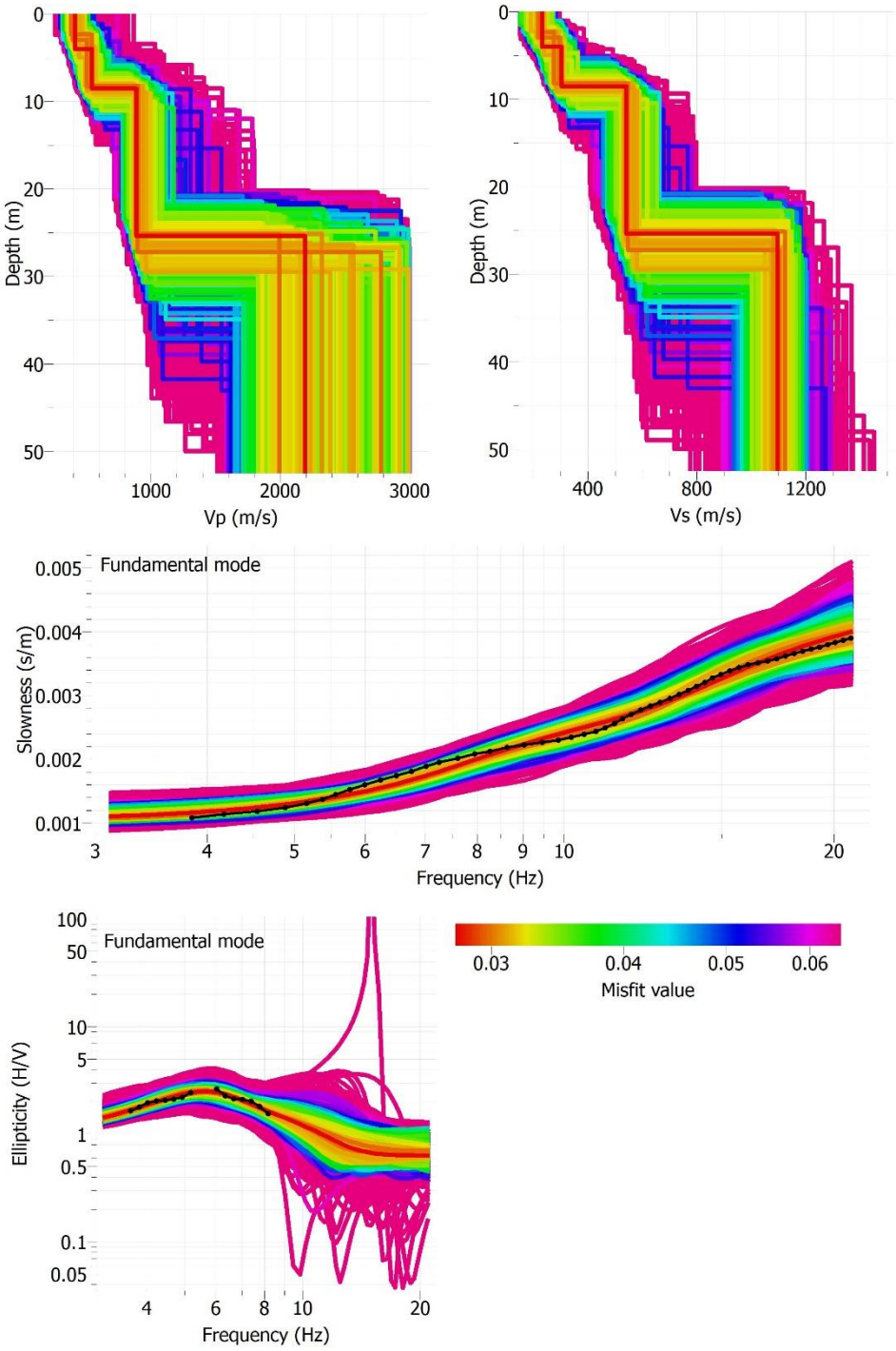

Figure 12: Inversion of the dispersion curve obtained with the 2D passive array, constrained with the H/V results (the field data are shown as black curves).

The best Vp and Vs model (i.e. lowest misfit) resulting from the inversion are proposed in Figure 13 and reported in Table 3.

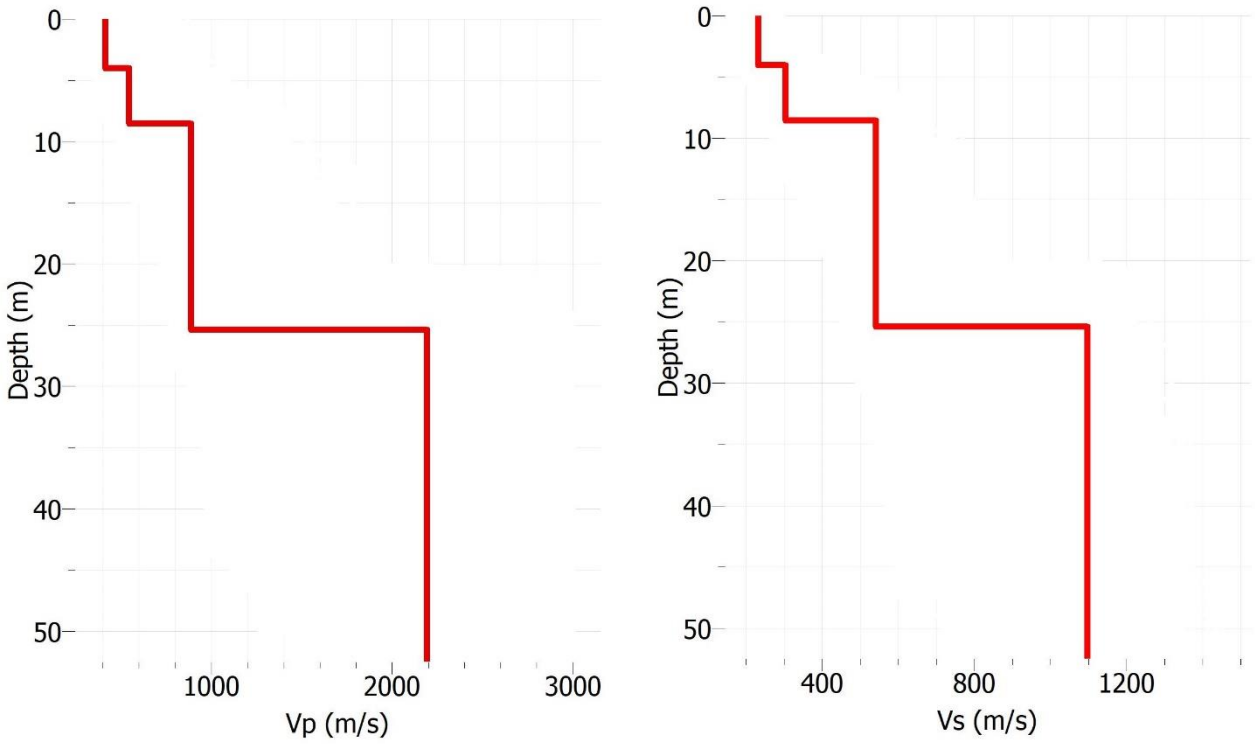

Figure 13: Best-fit models of Vp (left panel) and Vs (right panel) values.

From	*To*	*Thickness (m)*	*V_s (m/s)*	*V_p (m/s)*
0	4	4	231	413
4	8	8	305	544
8	25	17	536	878
25	?	?	1093	2188

Table 3: Best-fit model

4. CONCLUSIONS

The H/V analysis at the IV.VOBA seismic station indicates a resonant peak at 5.5 Hz, with a polarization effect between 80° and 160° (INGV-CRISP project, 2015-2016).

The Vs profile, obtained from the joint inversion of the Rayleigh wave dispersion curve and the H/V information, indicates soft layers (Vs ≤ 300) down to 8 m in depth, where *Vs* increases up to 536 m/s. The bedrock is found at 25 m in depth, with Vs > 800 m/s. This velocity discontinuity corresponds to the main seismic impedance contrast at the IV.VOBA site, constrained with the H/V peak at 5.5 Hz.

Figure 14 shows the correlation between geological and geophysical information at the study site. The increase in shear-wave velocity at 25 m in depth corresponds to the marly-limestone formation at the base of the fluvio-glacial deposits of Pleistocene age (Working group INGV (2019). Geological report at the seismic station IV. VOBA).

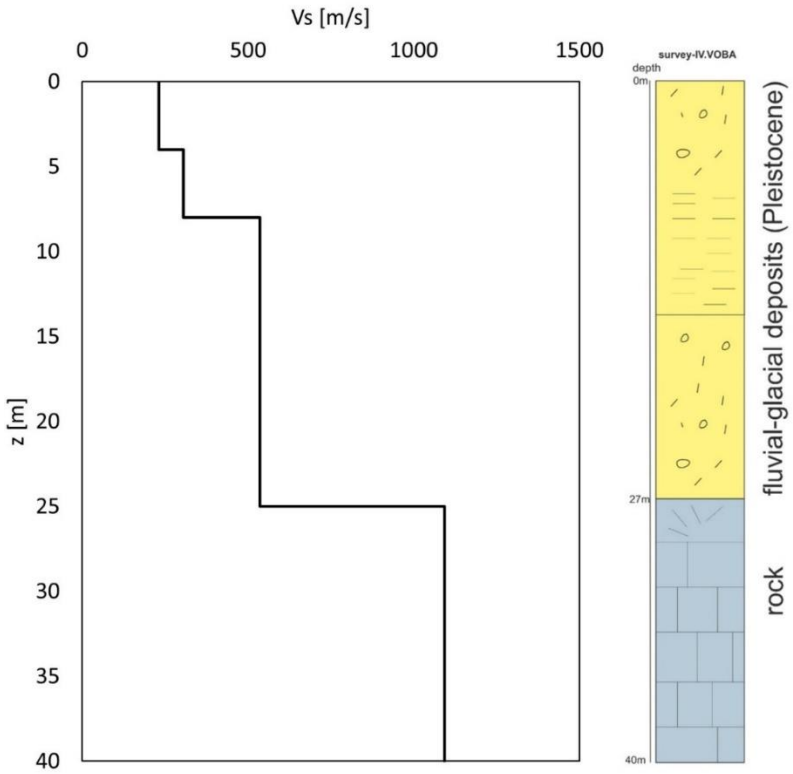

Figure 14: correlation between geological and geophysical information at the IV.VOBA site (stratigraphic column from Working group INGV (2019). Geological report at the seismic station IV. VOBA – Vobarno).

The $V_{S„eq}$ retrieved from the best inverted model is 332 m/s (Table 4), therefore IV.VOBA is classified in the soil category E following the NTC18 seismic classification. On the other hand, the $V_{S„30}$ retrieved from the best inverted model is 375 m/s (Table 4), therefore IV.VOBA is classified in the soil category B following the EC8 seismic classification.

$V_{s,eq}$ (m/s)	$V_{s,30}$ (m/s)	Soil class (NTC 2018)	Soil class (EC8)
332	375	E	B

Table 4: Soil Class

REFERENCES

EC8: European Committee for Standardization (2004). Eurocode 8: design of structures for earthquake resistance. P1: General rules, seismic actions and rules for buildings. Draft 6, Doc CEN/TC250/SC8/N335.

Foti, S., S. Parolai, D. Albarello, and M. Picozzi (2011). Application of surface-wave methods for seismic site characterization, Surv. Geophys. 32, no. 6, 777–825.

INGV-CRISP project, "CaRatterIzzazione dei sIti delle stazioni Sismiche Permanenti INGV" (Coordinators: Paola Bordoni e Giovanna Cultrera). Linea di attività INGV-T3 "Pericolosità sismica e contributi alla definizione del rischio", 2015-16; Convenzione DPC-INGV 2016-17-18, Allegato B2: Obiettivo 1 - TASK B: "Caratterizzazione siti accelerometrici".

NTC 2018: Ministero delle Infrastrutture e dei Trasporti (2018). Aggiornamento delle Norme Tecniche per le Costruzioni. Part 3.2.2: Categorie di sottosuolo e condizioni topografiche, Gazzetta Ufficiale n. 42 del 20 febbraio 2018 (in Italian).

Working group INGV "Agreement DPC-INGV 2019-21. All.B2 – WP1, Task 2", (2019). Geological report at the seismic station IV. VOBA - Vobarno. http://hdl.handle.net/2122/12909

Disclaimer and limits of use of information

The INGV, in accordance with the Article 2 of Decree Law 381/1999, carries out seismic and volcanic monitoring of the Italian national territory, providing for the organization of integrated national seismic network and the coordination of local and regional seismic networks as described in the agreement with the Department of Civil Protection.

INGV contributes, within the limits of its skills, to the evaluation of seismic and volcanic hazard in the Country, according to the mode agreed in the ten-year program between INGV and DPC February 2, 2012 (Prot. INGV 2052 of 27/2/2012), and to the activities planned as part of the National Civil Protection System.

In particular, this document1 has informative purposes concerning the observations and the data collected from the monitoring and observational networks managed by INGV.

INGV provides scientific information using the best scientific knowledge available at the time of the drafting of the documents produced; however, due to the complexity of natural phenomena in question, nothing can be blamed to INGV about the possible incompleteness and uncertainty of the reported data.

INGV is not responsible for any use, even partial, of the contents of this document by third parties and any damage caused to third parties resulting from its use.

The data contained in this document is the property of the INGV.

1This document is level 3 as defined in the "Principi della politica dei dati dell'INGV (D.P. n. 200 del 26.04.2016)"

Esclusione di responsabilità e limiti di uso delle informazioni

L'INGV, in ottemperanza a quanto disposto dall'Art.2 del D.L. 381/1999, svolge funzioni di sorveglianza sismica e vulcanica del territorio nazionale, provvedendo all'organizzazione della rete sismica nazionale integrata e al coordinamento delle reti sismiche regionali e locali in regime di convenzione con il Dipartimento della Protezione Civile.

L'INGV concorre, nei limiti delle proprie competenze inerenti la valutazione della Pericolosità sismica e vulcanica nel territorio nazionale e secondo le modalitaà concordate dall'Accordo di programma decennale stipulato tra lo stesso INGV e il DPC in data 2 febbraio 2012 (Prot. INGV 2052 del 27/2/2012), alle attività previste nell'ambito del Sistema Nazionale di Protezione Civile.

In particolare, questo documento1 ha finalità informative circa le osservazioni e i dati acquisiti dalle Reti di monitoraggio e osservative gestite dall'INGV.

L'INGV fornisce informazioni scientifiche utilizzando le migliori conoscenze scientifiche disponibili al momento della stesura dei documenti prodotti; tuttavia, in conseguenza della complessità dei fenomeni naturali in oggetto, nulla può essere imputato all'INGV circa l'eventuale incompletezza ed incertezza dei dati riportati.

L'INGV non è responsabile dell'utilizzo, anche parziale, dei contenuti di questo documento da parte di terzi e di eventuali danni arrecati a terzi derivanti dal suo utilizzo.

La proprietà dei dati contenuti in questo documento è dell'INGV.

1Questo documento rientra nella categoria di livello 3 come definita nei "Principi della politica dei dati dell'INGV (D.P. n. 200 del 26.04.2016)".